



# Acyldepsipeptide Probes Facilitate Specific Detection of Caseinolytic Protease P Independent of Its Oligomeric and Activity State

Barbara Eyermann,<sup>[a]</sup> Maximilian Meixner,<sup>[b]</sup> Heike Brötz-Oesterhelt,<sup>[c]</sup> Iris Antes,<sup>[b]</sup> and Stephan A. Sieber\*<sup>[a]</sup>

Caseinolytic protease P (ClpP) is a tetradecameric peptidase that assembles with chaperones such as ClpX to gain proteolytic activity. Acyldepsipeptides (ADEPs) are small-molecule mimics of ClpX that bind into hydrophobic pockets on the apical site of the complex, thereby activating ClpP. Detection of ClpP has so far been facilitated with active-site-directed probes which depend on the activity and oligomeric state of the complex. To expand the scope of ClpP labeling, we took a stepwise synthetic approach toward customized ADEP photo-

probes. Structure–activity relationship studies with small fragments and ADEP derivatives paired with modeling studies revealed the design principles for suitable probe molecules. The derivatives were tested for activation of ClpP and subsequently applied in labeling studies of the wild-type peptidase as well as enzymes bearing mutations at the active site and an oligomerization sensor. Satisfyingly, the ADEP photoprobes provided a labeling readout of ClpP independent of its activity and oligomeric state.

## Introduction

ClpP, the proteolytic core of the caseinolytic protease, is a barrel-shaped serine peptidase composed of two heptameric rings which assemble into a tetradecameric complex (Figure 1A,B).<sup>[1,2]</sup> Several structural studies have shown that the enzyme samples various conformations including an active extended state with an elongated central helix and an aligned catalytic triad as well as a compressed state with a fully kinked helix and a misaligned triad.<sup>[3,4]</sup> In addition, a compact state representing a transition between the two has been observed.<sup>[3,5–7]</sup> Several crucial residues within ClpP have been identified which support the oligomeric state and corresponding activity. For example, an oligomerization sensor between Asp170 and Arg171 forms crucial contacts between the hepta-

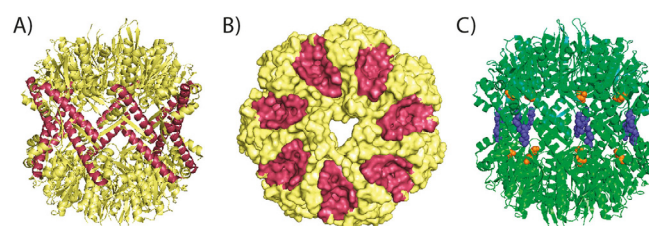




**Figure 1.** Structure of tetradecameric SaClpP depicted in the A) side view with marked central helix (red) and in the B) top view, with marked hydrophobic pockets (red). C) SaClpP with the marked amino acids S98 (orange) and R171 (blue) (PDB ID: 3STA).


[a] B. Eyermann, Prof. Dr. S. A. Sieber  
Department Chemie, Technische Universität München  
Lichtenbergstrasse 4, 85748 Garching (Germany)  
E-mail: stephan.sieber@tum.de

[b] M. Meixner, Prof. Dr. I. Antes  
Department für Biowissenschaften, Technische Universität München  
Emil-Erlenmeyer-Forum 8, 85354 Freising (Germany)

[c] Prof. Dr. H. Brötz-Oesterhelt  
Interfaculty Institute of Microbiology and Infection Medicine  
Microbial Bioactive Compounds, University of Tübingen  
Auf der Morgenstelle 28, E-Bau, Ebene 8, 72076 Tübingen (Germany)

 Supporting information and the ORCID identification numbers for the authors of this article can be found under <https://doi.org/10.1002/cbic.201900477>.

 © 2019 The Authors. Published by Wiley-VCH Verlag GmbH & Co. KGaA. This is an open access article under the terms of the Creative Commons Attribution Non-Commercial License, which permits use, distribution and reproduction in any medium, provided the original work is properly cited and is not used for commercial purposes.

 This article is part of a Special Issue commemorating the 20th Anniversary of ChemBioChem. To view the complete issue, visit our homepage

mer–heptamer interface and ensures a stable tetradecameric complex.<sup>[4,8]</sup> Mutations of either of the two residues results in complex disassembly into inactive heptamers. Overall, these previous studies demonstrated that the conformational state of the complex and its corresponding enzymatic activity are directly linked.<sup>[4,9]</sup>

ClpP digests small peptide chains, but is unable to act on larger proteins due to the restricted pore size of the proteolytic chamber. For the degradation of these proteins, the complex binds to chaperones such as ClpX which assist in ATP-dependent unfolding and threading the linear peptide chain into the ClpP barrel.<sup>[10–13]</sup> ClpX uses IGF peptide loops to specifically dock into cognate hydrophobic pockets on the apical site of ClpP.<sup>[14]</sup> Natural product acyldepsipeptides (ADEPs) represent small-molecule mimics of these IGF loops which address the same binding site and thereby induce opening of the central pore to facilitate access of larger substrates.<sup>[15–17]</sup> This uncontrolled access and digestion of cellular proteins results in dysregulation of protein homeostasis and corresponding antibiotic

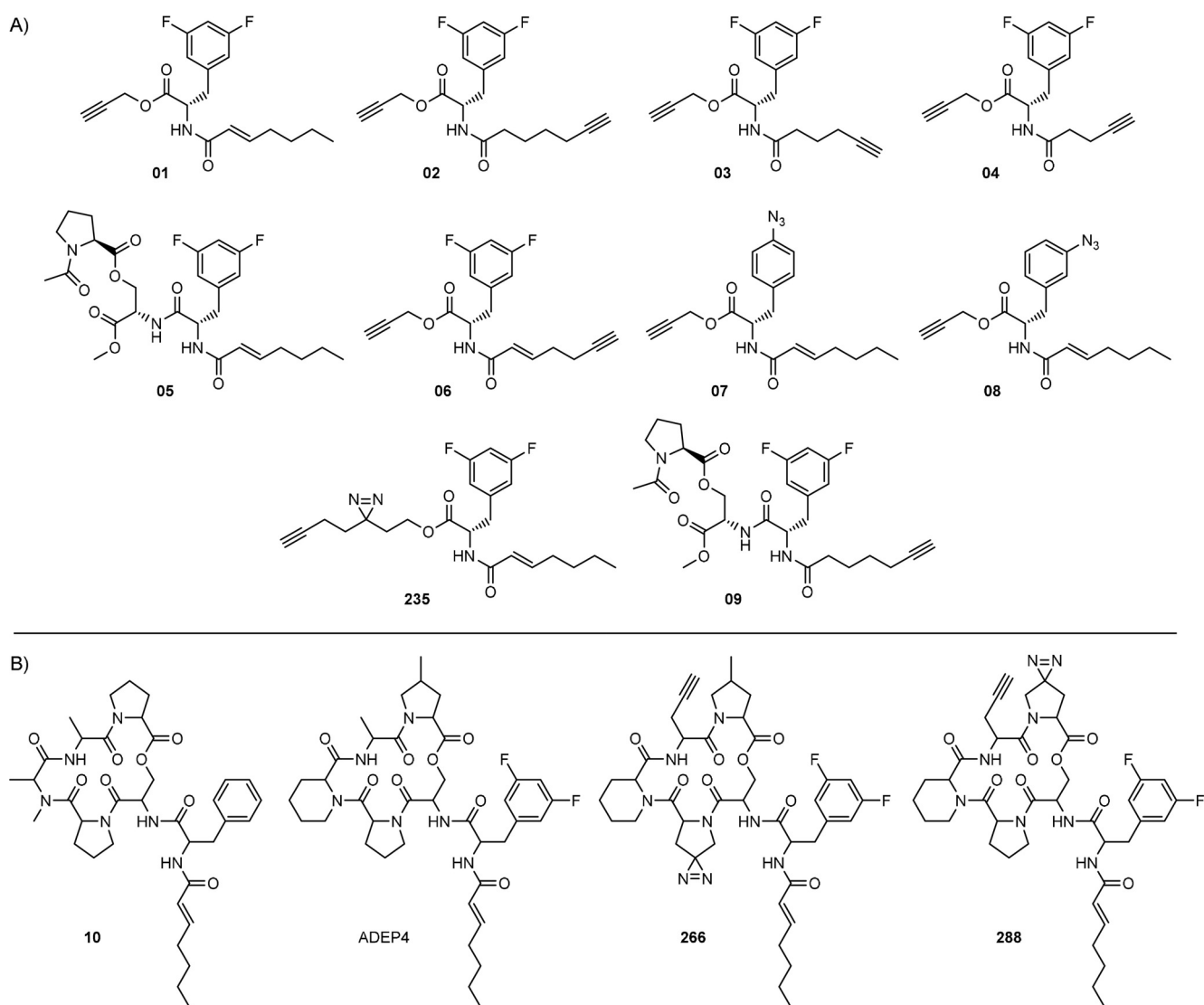
activity against for example *Staphylococcus aureus* and its persistent strains.<sup>[18,19]</sup>

In addition to activation, natural product derived  $\beta$ -lactones were shown to acylate the active site and thereby inhibit enzymatic turnover. The consequence of this mechanism is a decrease in *S. aureus* virulence. Alkynylated probes of  $\beta$ -lactones or other active site inhibitors have been used to readout the activity state of ClpP in various settings including living cells.<sup>[20,21]</sup> While these probes require an aligned active site for acylation, they solely detect ClpP in its active state, but are blind for other inactive conformations. Despite intensive studies on ClpP labeling, probes to target an activity-independent allosteric site have not yet been introduced. To obtain complementary probes for detecting ClpP in various conformational states, we here exploited IGF loop mimics for binding into the hydrophobic pocket and their readout on different ClpP mutants.

## Results and Discussion

### ADEP probe design and synthesis

To design novel probes for ClpP affinity-based protein profiling (AfBPP), ADEP derivatives need to be functionalized with an alkyne handle as well as a photoreactive group.<sup>[22–24]</sup> The photo-crosslinker forms a covalent bond with amino acid residues in the proximity of the binding site upon UV irradiation and subsequent modification of the alkyne with an azide tag via click chemistry allows visualization and detection. Ideally, these moieties need to be introduced at positions that do not affect the compounds' binding to the hydrophobic pockets of ClpP. Previous structure–activity relationship studies (SAR) with ADEPs revealed that small fragments containing the *N*-acyldi-fluorophenylalanine moiety retain ClpP activation and antibiotic activity albeit with lower potency than the full-length depsipeptides.<sup>[25]</sup> Moreover, derivatives lacking an unsaturated bond



**Scheme 1.** Structures of A) different ADEP fragments, with published structures 01<sup>[25]</sup> and 05<sup>[25]</sup> and fragment photoprobe 235 and B) ADEP derivatives 10,<sup>[26]</sup> ADEP4, and photoprobes 266 and 288.

next to the amide in the alkyl chain were nearly inactive. Several ADEP fragments were designed to decipher if other modifications are tolerated at this moiety. These included variations in the length of the side chain, introduction of an alkyne, the deletion of the double bond and an aryl azide at the phenyl alanine moiety.<sup>[25]</sup> Starting from compound **01**, previously introduced by Sello and co-workers,<sup>[25]</sup> we first tested if an alkyne handle would be accepted at the terminal end of the acyl chain. Most of the fragments, **02**, **03**, **04**, and **06**, were easily accessible via an esterification, followed by Boc deprotection and amide coupling (Scheme 1A, Scheme S1B in the Supporting Information). The two larger fragments **05** and **09** were synthesized via a four-step synthetic route, depicted in Scheme S1A (Scheme 1A).

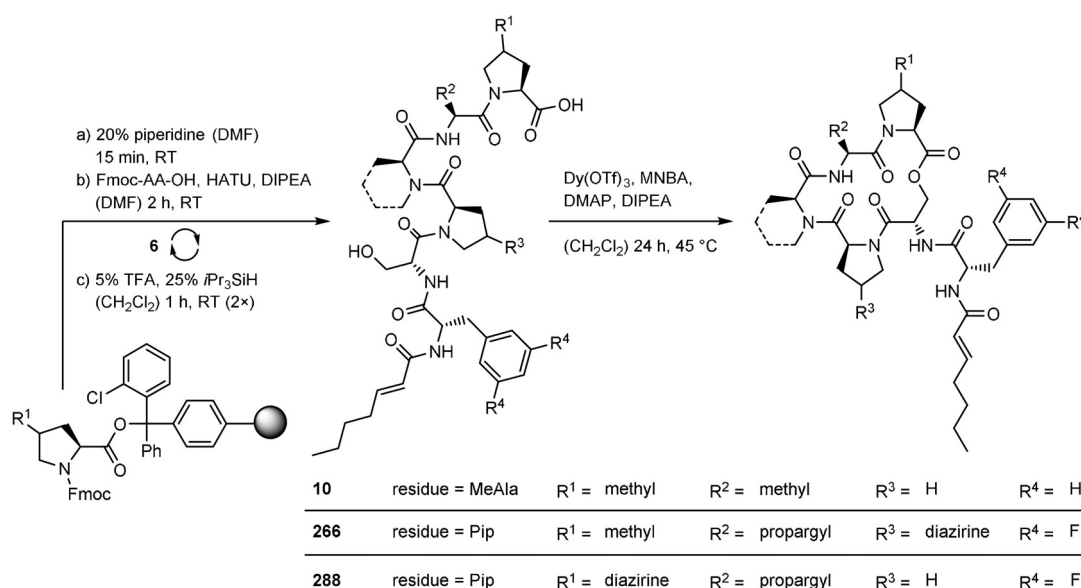
To rank the corresponding activities of all derivatives we performed ClpP activity assays with FITC-casein as a substrate.<sup>[27,28]</sup> In the absence of an activator the small ClpP pore prevents access of the substrate, while activator binding opens the channel and allows processing. Compound **01** was used as an internal control. As expected, derivatives **02**, **03**, **04** and **09** with varying alkyne chain lengths but which lack the crucial amide double bond, were found to be inactive (Figure 3A). To our surprise, even in presence of the crucial double bond, compound **06** did not gain any activity, demonstrating that the introduction of an alkyne at the acyl chain is not tolerated.

To exploit other putative modifications, we prepared aryl azides **07** and **08** starting from Boc-protected phenylalanine with bromide in the *para* position and nitro group in the *meta* position, respectively. The introduction of an azide yielded two possible photoprobes (Schemes 1A and S2). Activity tests with these probes revealed that neither the *para* (**07**) nor *meta* (**08**) positioned azide showed any activating effect, highlighting again the restricted flexibility in this crucial fragment (Figure 3A). Finally, a minimal alkyne chain equipped with a diazirine photo-crosslinker on the western side of the molecule (**235**) resulted in about 90% activation relative to the starting

compound, yielding the first functional fragment probe (Figure 3A, Schemes 1A and S1B).

To further improve the activity, we aimed to design a probe that is based on the whole ADEP scaffold. Here, based on the previous experience with fragments, modifications were deliberately made solely at the macrocyclic core, that is, at the alanine and one of the two proline residues. Starting from the structure of ADEP4, we designed two probes with an alkyne modified alanine and either a photoproline in the southern position (**266**) or the northern position (**288**; Scheme 1B). The synthesis of these probes was executed by using solid-phase peptide synthesis with subsequent ring-closure reaction. First, Fmoc-protected methylproline (**11**), Fmoc-protected photoproline (**12**) and Fmoc-protected pipecolic acid (**13**) were prepared, as depicted in Scheme S3. The first amino acid, methylproline in case of **266** and photoproline in case of **288**, was loaded on the resin, followed by the coupling of Fmoc-protected propargylglycine, pipecolic acid, photoproline or proline, serine, phenylalanine derivative and heptenoic acid. Ring closure was achieved by lactonization, with the method published by Batey and co-workers in 2015 (Schemes 2 and S4).<sup>[29]</sup> Final activity studies of the two ADEP probes revealed that **266** was a significantly better activator of ClpP (150% relative to internal control) than **288**, which only achieved around 30% (Figure 3A). ADEP4 and compound **10**, a derivative lacking the fluorine atoms at the phenylalanine, the methyl group at the proline and the pipecolic acid moiety, were included as controls. They also achieved maximum activation similar to the most active **266** probe, albeit at much lower concentrations in the case of ADEP4, emphasizing its higher affinity and better fit into the hydrophobic pocket (Figure S1).

Modeling of the probes into the hydrophobic pocket provided a rational explanation for the observed differences in activation. In Figure 2 the modeled positions and orientations of **266** and **288** are shown together with the crystal structures of co-crystallized ADEPs (Figure 2C, D, Scheme S4A). While the over-



**Scheme 2.** Synthetic route for the synthesis of ADEP derivatives **10**, **266**, and **288**.

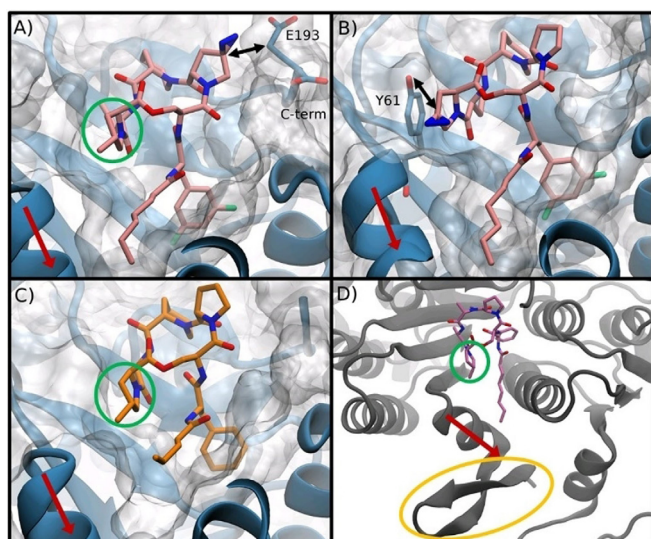


**Figure 2.** Most prominent docked poses of ligands A) **266** and B) **288** and X-ray structures of bound ADEP (structure in Figure S3 A) in *SaClpP* (C, PDB ID: 5VZ2) and ADEP1 in *EcClpP* (D, PDB ID: 3MT6). Ligands are shown in stick representation, and proteins are illustrated as cartoons. Red arrows mark the position of the  $\alpha$ -helix important for propagating structural changes to the  $\beta$ -sheet loops (yellow circle in panel D) at the edge of the pore. Methylproline is highlighted with a green circle. Residues closest to the photoproline moiety (indicated with black arrows) are shown as sticks for **266** and **288**. Atom color scheme: nitrogen, dark blue; oxygen, red; fluorine, green; carbon, other.

all binding mode is conserved for all molecules there are distinct differences, especially with respect to a signature methylproline moiety (green circle in Figure 2), which was found to be important for the activation mechanism of ClpP.<sup>[17]</sup> In the case of **266**, this moiety is located at the same position as in the experimental structures of ADEPs suggesting a similar mechanism of binding and activation (Figure 2A versus C,D). However, in **288** the diazirine moiety, replacing the methyl group, induces a shift of the macrocycle, such that the photocrosslinker points inside the binding site close to for example, Y61, which could explain the observed strong and stable labeling. In contrast, in **266** the reactive diazirine moiety points toward the solvent and is located close to the flexible C termi-

nus, in line with a weaker labeling signal (for further modelling data of derivatives, please refer to Figure S4).

### Biological activity and labeling of ClpP in living cells

All ClpP-activating compounds were tested for their antibiotic activities against *S. aureus* cells and corresponding minimal inhibitory concentrations (MIC) were determined. Compound **01** served again as control with a MIC value of  $20.0 \mu\text{M}$  ( $\pm 6.12 \mu\text{M}$ ).<sup>[25]</sup> While ADEP4 exhibited the highest potency with  $< 15 \text{ nM}$ , compounds **266** and **10** showed, in agreement with ClpP activation, moderate MICs of  $3.09 \pm 0.06 \mu\text{M}$  and  $4.35 \pm 2.33 \mu\text{M}$ , respectively. This again highlights that their structural perturbations compromised the overall activity; however, they were sufficient to retain antibiotic effects. In contrast **288** was inactive at the concentrations tested, reflecting its rather weak activation of ClpP. Surprisingly, probe **235** was also inactive despite a good activation of ClpP similar to **01** (Table S1).

To investigate if the bioactivity correlates with labeling of ClpP, we performed AfBPP studies with **235**, **266**, and **288**. Purified *SaClpP* was incubated with  $10 \mu\text{M}$  probe, irradiated and clicked to a fluorescence tag. Importantly, as predicted **288** protruded as a strong labeling probe exceeding the performance of **266** (Figure S1 B). Further studies with ADEP4 demonstrated, that the **288** probe signal vanishes with increasing concentration of a competitor, suggesting that both compounds address the same binding pocket (Figure 3 B). Labeling could also be shown in situ with intact *S. aureus* cells in the stationary phase. Probes were incubated for short time points of 1 h in order to minimize cell killing. The most prominent band was confirmed to be ClpP via western blot with the respective antibody and the labeling in a clpP knockout strain resulted in a lack of the characteristic band (Figure S2 B,C). Furthermore, ClpP could be identified in an LC-MS/MS-based AfBPP workflow (Figure S5). These results highlight the required specificity of the probe for its target.

### Labeling of ClpP in different conformational states

To determine if ClpP can be labeled in different conformational states, we overexpressed and purified an active-site mutant

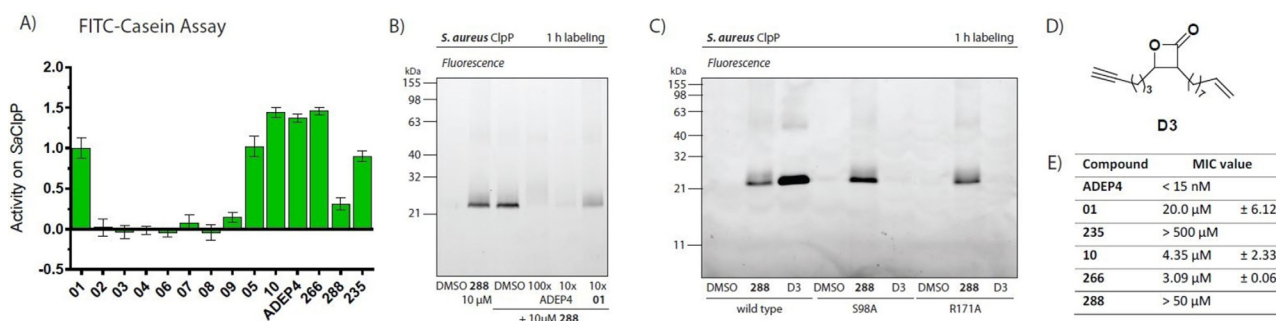


**Figure 3.** A) FITC-casein activity assay of several ADEP fragments and derivatives. Shown is the activity on *SaClpP* at a concentration of  $20 \mu\text{M}$ , normalized to the internal standard **01**. Experiments were carried out in triplicates. B) Labeling of recombinant *SaClpP* with photoprobe **288** and ADEP4 and **01** as competitors. Competitor and probe were added at the same time and incubated for one hour. C) Labeling of *SaClpP* wild-type and mutants, S98A and R171A, with photoprobe **288** in comparison with  $\beta$ -lactone **D3** at a concentration of  $10 \mu\text{M}$ . D) Structure of **D3**. E) MIC values of ADEP fragments and derivatives in *S. aureus* NCTC8325.

(S98A) and a disrupted oligomerization mutant (R171A), together with the wild-type enzyme as control (Figure 1 C). These proteins were subsequently labeled with the **288** probe and an active-site-directed  $\beta$ -lactone (**D3**) as benchmark control. Interestingly, while **288** detected wild-type and both mutants, the **D3** signal was only obtained for the active wild-type (Figure 3 C,D). In line with our hypothesis, these results establish **288** as a conformation-independent probe for selective and universal ClpP detection.

## Conclusion

We here introduce a complementary chemical tool for the selective detection of ClpP that goes beyond active site labeling of previously introduced probes. SAR studies not only guided the design of ADEP probes but also provided more general aspects of binding into the hydrophobic pocket which was further elucidated by molecular docking. Overall, only limited structural modifications were tolerated but still resulted in a significant drop of activity which challenged the design of photo-crosslinker probes.

Here the linker either retains higher activity but points outward of the pocket or is inside but clashes with the binding site. However, as **288** serves as a suitable detection tool, the reduced activity is acceptable, and sufficient labeling could still be observed *in vitro* and *in situ*, suggesting that the probe has great potential for applications to monitor ClpP, in its active and inactive conformational states.

## Experimental Section

**Synthesis of fragment photoprobe 235:** *N*-Boc-3,5-difluorophenylalanine (50.0 mg, 166  $\mu\text{mol}$ , 1.0 equiv) and minimal photo-crosslinker **32** (22.9 mg, 166  $\mu\text{mol}$ , 1.0 equiv) were dissolved in  $\text{CH}_2\text{Cl}_2$  (1.5 mL) and EDC-HCl (38.2 mg, 199  $\mu\text{mol}$ , 1.2 equiv) and DMAP (1.01 mg, 8.30  $\mu\text{mol}$ , 0.1 equiv) were added. The reaction was stirred at room temperature for 2.5 h, the solvent was removed under reduced pressure, the residue was taken up in ethyl acetate (2.0 mL) and was washed with 1 M HCl, sat.  $\text{NaHCO}_3$  and sat. NaCl solutions, 2.0 mL each. A crude product (63.3 mg) was obtained and used for deprotection of the Boc group without further purification.

For Boc deprotection, the crude product was dissolved in 40% TFA in  $\text{CH}_2\text{Cl}_2$  (1.5 mL) and stirred for 1.5 h. Argon was forced over the reaction to evaporate the solvent.

For the amide synthesis, *E*-2-heptenoic acid (21.0  $\mu\text{L}$ , 96.0  $\text{mg mL}^{-1}$ , 154  $\mu\text{mol}$ , 1.0 equiv) was dissolved in DMF (1.0 mL), HATU (64.0 mg, 169  $\mu\text{mol}$ , 1.1 equiv) and DIPEA (59.0  $\mu\text{L}$ , 742  $\text{mg mL}^{-1}$ , 339  $\mu\text{mol}$ , 2.2 equiv) were added and the reaction was stirred for 15 min. Subsequently the crude amino acid in DMF (0.5 mL) was added and the mixture was stirred for 24 h. The reaction mixture was diluted with ethyl acetate (7.5 mL) and was washed with 1 M HCl, sat.  $\text{NaHCO}_3$  and sat. NaCl solutions, 2.0 mL each. The organic layer was dried over  $\text{Na}_2\text{SO}_4$  and the solvent was removed under reduced pressure. A light-yellow solid (28.6 mg, 43% over three steps) was obtained after purification with column chromatography (hexane/ethyl acetate 5:1 to 3:1). For analytical data, please see the Supporting Information, Chapter 4.3.

**Synthesis of ADEP-photoprobe 266:** 2-chlorotriyl chloride resin (503 mg) was loaded with Fmoc-proline derivative **11** (126 mg, 359  $\mu\text{mol}$ ), to obtain a loading of 473  $\mu\text{mol g}^{-1}$  (general procedure D). Following amino acids were coupled to the resin using general procedures E, F and G: Fmoc-propargylglycine (158 mg, 473  $\mu\text{mol}$ ), Fmoc-pipecolic acid (170 mg, 473  $\mu\text{mol}$ ), Fmoc-photopline **12** (124 mg, 341  $\mu\text{mol}$ ), Fmoc-serine (154 mg, 473  $\mu\text{mol}$ ), Fmoc-3,5-difluorophenylalanine (129 mg, 306  $\mu\text{mol}$ ) and *E*-2-heptenoic acid (63.4  $\mu\text{L}$ , 950  $\text{mg mL}^{-1}$ , 473  $\mu\text{mol}$ ). The heptapeptide was cleaved of the resin using general procedure H. (yield: 76% over six coupling steps) The cyclization was performed according to general procedure I, using the resulting heptapeptide (10.0 mg, 11.9  $\mu\text{mol}$ , 1.0 equiv), MNBA (12.3 mg, 35.7  $\mu\text{mol}$ , 3.0 equiv), DIPEA (5.68  $\mu\text{L}$ , 742  $\text{mg mL}^{-1}$ , 33.4  $\mu\text{mol}$ , 2.8 equiv), DMAP (8.70 mg, 71.5  $\mu\text{mol}$ , 6.0 equiv) and  $\text{Dy}(\text{OTf})_3$  (7.30 mg, 11.9  $\mu\text{mol}$ , 1.0 equiv). The crude product was purified by reversed phase HPLC (ACN/ $\text{H}_2\text{O}$ ; ACN 2% to 60%). Yield: 8.34 mg (85%). For general procedures and analytical data, please see the Supporting Information, Chapters 4.5 and 5.6.

**Synthesis of ADEP-photoprobe 288:** 2-chlorotriyl chloride resin (559 mg) was loaded with Fmoc-photopline (110 mg, 303  $\mu\text{mol}$ ), to obtain a loading of 400  $\mu\text{mol g}^{-1}$  (general procedure D). Following amino acids were coupled to the resin using general procedures E, F and G: Fmoc-propargylglycine (172 mg, 510  $\mu\text{mol}$ ), Fmoc-pipecolic acid (181 mg, 510  $\mu\text{mol}$ ), Fmoc-proline (173 mg, 510  $\mu\text{mol}$ ), Fmoc-serine (177 mg, 510  $\mu\text{mol}$ ), Fmoc-3,5-difluorophenylalanine (218 mg, 510  $\mu\text{mol}$ ) and *E*-2-heptenoic acid (69.4  $\mu\text{L}$ , 950  $\text{mg mL}^{-1}$ , 510  $\mu\text{mol}$ ). The heptapeptide was cleaved of the resin using general procedure H. (Yield: 22% over six coupling steps) The cyclization was performed according to general procedure I, using the resulting heptapeptide (50.0 mg, 60.6  $\mu\text{mol}$ , 1.0 equiv), MNBA (62.6 mg, 182  $\mu\text{mol}$ , 3.0 equiv), DIPEA (28.9  $\mu\text{L}$ , 760  $\text{mg mL}^{-1}$ , 170  $\mu\text{mol}$ , 2.8 equiv), DMAP (44.4 mg, 364  $\mu\text{mol}$ , 6.0 equiv) and  $\text{Dy}(\text{OTf})_3$  (37.0 mg, 60.6  $\mu\text{mol}$ , 1.0 equiv). The crude product was purified by reversed-phase HPLC (ACN/ $\text{H}_2\text{O}$ ; ACN 2% to 98%). Yield: 3.05 mg (6%). For general procedures and analytical data, please see the Supporting Information, Chapters 4.5. and 5.6.

**FITC-casein assay:**<sup>[27,28]</sup> The aim of this assay was to determine the proteolytic activity of ClpP with different compounds. For the FITC-casein assay, 100  $\mu\text{L}$  sample was prepared in a black 96-well plate, with a concentration of 1  $\mu\text{M}$  ClpP and different final concentrations of the compound. Compound **01** was used as positive control with a concentration of 20  $\mu\text{M}$  and DMSO as a negative control. All set ups were carried out in triplicates; 1  $\mu\text{L}$  DMSO or compound in DMSO was placed in each well and 80  $\mu\text{L}$  ClpP in buffer (1.25  $\mu\text{M}$ , in PZ buffer: 25 mM HEPES, 200 mM KCl, 5 mM  $\text{MgCl}_2$ , 1 mM DTT, 10% glycerol, pH 7.6) was added. After incubation at 37  $^\circ\text{C}$  for 15 min, 20  $\mu\text{L}$  of substrate (2 mM FITC-casein, 10 mM casein, in PBS) was added to each probe. After excitation at 485 nm, the fluorescence emission was measured by a Tecan infinite F200 Pro at 535 nm. Initial slopes over time were evaluated by a linear regression model, and all values were normalized to the **01** control, after subtraction of the DMSO control.

**Labeling of recombinant protein:** 0.5  $\mu\text{L}$  DMSO or compound (1:100, different concentrations in DMSO) was placed in a transparent 96-well plate and 44  $\mu\text{L}$  SaClpP in PBS (final concentration 2  $\mu\text{M}$ ) was added. After incubation for one hour in the dark, the mixture was irradiated for 10 min at 365 nm (Philips TL-DBLB18W), 5  $\mu\text{L}$  gel-based click reagent mix [1  $\mu\text{L}$   $\text{RhN}_3$  (TAMRA azide, 5 mM in DMSO), 1  $\mu\text{L}$  freshly prepared TCEP (50 mM in  $\text{ddH}_2\text{O}$ ), 3  $\mu\text{L}$  TBTA ligand (1.67 mM in 80% *t*BuOH and 20% DMSO)] and 1  $\mu\text{L}$  50 mM  $\text{CuSO}_4$  were added and incubated for 1 h in the dark. Then 50  $\mu\text{L}$

2× Laemmli sample buffer (63 mM Tris-HCl, 10% glycerol, 2% SDS, 0.0025% Bromophenol Blue, 5% 2-mercaptoethanol) were added and the samples analyzed via SDS-PAGE [12.5% or 15% agarose gel, 2.5 h, 150 V, 8 μL fluorescent protein standard, fluorescence imaging (GE Healthcare, ImageQuant LAS-4000)].

**Computational studies:** For all modeling studies the X-ray structure PDB ID: 5VZ2 (ClpP from *S. aureus* + acyldepsipeptide) of the SaClpP protein with bound ADEP was used. The modeling procedure applied is based on a molecular dynamics-based docking pipeline, which was previously developed and optimized specifically for the docking of macrocyclic compounds.<sup>[30]</sup> It contains the following steps: I) Conformational sampling of the compounds in aqueous solution, clustering and extraction of the most prominent conformations of the macrocycle. II) Equilibrium molecular dynamics simulations of the experimental structure of the protein–ligand complex (PDB ID: 5VZ2). III) Fully flexible molecular dynamics-based docking of all compound conformations obtained from (I) into the equilibrated binding site from (II). For the steps (I) and (II) the program Amber17 was used.<sup>[31]</sup> All molecular docking calculations were performed with the DynaDock program.<sup>[32]</sup> In addition, to evaluate the performance of the pipeline and optimize its parameters for the molecular system at hand, first re-docking experiments of the co-crystallized ADEP molecule (Figure 2C) into its binding site in SaClpP were performed using the equilibrated PDB ID: 5VZ2 protein–ligand complex. With the docking pipeline presented herein, a binding pose of the ADEP molecule with a root-mean-square deviation (RMSD) of 1.6 Å for all non-hydrogen ligand atoms (data not shown) from those of the equilibrated holo-structure (ClpP<sup>5VZ2</sup>) could be obtained, thereby assuring the suitability of the procedure for docking studies of the SaClpP–ligand system. The so-optimized and validated docking parameters were afterward applied for the prediction of the bound conformations of compounds **266** and **288** into the same SaClpP protein structure. A detailed description of the computational conditions and parameters applied is provided in the Supporting Information, Chapter 3.

## Acknowledgements

The mass spectrometry proteomics data have been deposited at the ProteomeXchange Consortium via the PRIDE<sup>[33]</sup> partner repository with the dataset identifier PXD015244. The work was funded by the Deutsche Forschungsgemeinschaft (DFG) SFB1035 and SFB766 and the Center for Integrated Protein Science Munich (CIPSM). We thank Patrick Allihn for the ClpP mutants, Christian Fetzner for the *S. aureus* NCTC8325 clpP knockout strain, and Thomas Gronauer for D3. We also thank Mona Wolff, Katja Bäuml, Katja Gliesche, and Drazen Jalsovec for excellent technical support.

## Conflict of Interest

The authors declare no conflict of interest.

**Keywords:** acyldepsipeptides · antibiotics · caseinolytic protease P · photoaffinity labeling · virulence

[1] M. Kessel, M. R. Maurizi, B. Kim, E. Kocsis, B. L. Trus, S. K. Singh, A. C. Steven, *J. Mol. Biol.* **1995**, *250*, 587–594.

- [2] S. Gottesman, E. Roche, Y. N. Zhou, R. T. Sauer, *Genes Dev.* **1998**, *12*, 1338–1347.
- [3] S. R. Geiger, T. Böttcher, S. A. Sieber, P. Cramer, *Angew. Chem. Int. Ed.* **2011**, *50*, 5749–5752; *Angew. Chem.* **2011**, *123*, 5867–5871.
- [4] M. Gersch, A. List, M. Groll, S. A. Sieber, *J. Biol. Chem.* **2012**, *287*, 9484–9494.
- [5] F. Ye, J. Zhang, H. Liu, R. Hilgenfeld, R. Zhang, X. Kong, L. Li, J. Lu, X. Zhang, D. Li, H. Jiang, C.-G. Yang, C. Luo, *J. Biol. Chem.* **2013**, *288*, 17643–17653.
- [6] J. Zhang, F. Ye, L. Lan, H. Jiang, C. Luo, C.-G. Yang, *J. Biol. Chem.* **2011**, *286*, 37590–37601.
- [7] B. G. Lee, M. K. Kim, H. K. Song, *Mol. Cells* **2011**, *32*, 589–595.
- [8] M. Stahl, S. A. Sieber, *Curr. Opin. Chem. Biol.* **2017**, *40*, 102–110.
- [9] I. T. Malik, H. Brötz-Oesterhelt, *Nat. Prod. Rep.* **2017**, *34*, 815–831.
- [10] W. F. Wu, Y. Zhou, S. Gottesman, *J. Bacteriol.* **1999**, *181*, 3681–3687.
- [11] S. Gottesman, *Annu. Rev. Genet.* **1996**, *30*, 465–506.
- [12] J. Wang, J. A. Hartling, J. M. Flanagan, *Cell* **1997**, *91*, 447–456.
- [13] C. K. Smith, T. A. Baker, R. T. Sauer, *Proc. Natl. Acad. Sci. USA* **1999**, *96*, 6678–6682.
- [14] D. Y. Kim, K. K. Kim, *J. Biol. Chem.* **2003**, *278*, 50664–50670.
- [15] J. Kirstein, A. Hoffmann, H. Lillie, R. Schmidt, H. Rübbsamen-Waigmann, H. Brötz-Oesterhelt, A. Mogk, K. Turgay, *EMBO Mol. Med.* **2009**, *1*, 37–49.
- [16] B.-G. Lee, E. Y. Park, K.-E. Lee, H. Jeon, K. H. Sung, H. Paulsen, H. Rübbsamen-Schaeff, H. Brötz-Oesterhelt, H. K. Song, *Nat. Struct. Mol. Biol.* **2010**, *17*, 471–478.
- [17] D. H. S. Li, Y. S. Chung, M. Gloyd, E. Joseph, R. Ghirlando, G. D. Wright, Y.-Q. Cheng, M. R. Maurizi, A. Guarné, J. Ortega, *Chem. Biol.* **2010**, *17*, 959–969.
- [18] H. Brötz-Oesterhelt, D. Beyer, H. P. Kroll, R. Endermann, C. Ladell, W. Schroeder, B. Hinzen, S. Raddatz, H. Paulsen, K. Henninger, J. E. Bandow, H.-G. Sahl, H. Labischinski, *Nat. Med.* **2005**, *11*, 1082–1087.
- [19] B. P. Conlon, E. S. Nakayasu, L. E. Fleck, M. D. LaFleur, V. M. Isabella, K. Coleman, S. N. Leonard, R. D. Smith, J. N. Adkins, K. Lewis, *Nature* **2013**, *503*, 365–370.
- [20] T. Böttcher, S. A. Sieber, *J. Am. Chem. Soc.* **2008**, *130*, 14400–14401.
- [21] T. Böttcher, S. A. Sieber, *Angew. Chem. Int. Ed.* **2008**, *47*, 4600–4603; *Angew. Chem.* **2008**, *120*, 4677–4680.
- [22] M. J. Evans, B. F. Cravatt, *Chem. Rev.* **2006**, *106*, 3279–3301.
- [23] D. J. Lapinsky, *Bioorg. Med. Chem.* **2012**, *20*, 6237–6247.
- [24] P. P. Geurink, L. M. Prely, G. A. van der Marel, R. Bischoff, H. S. Overkleeft, *Top. Curr. Chem.* **2011**, *324*, 85–113.
- [25] D. W. Carney, C. L. Compton, K. R. Schmitz, J. P. Stevens, R. T. Sauer, J. K. Sello, *ChemBioChem* **2014**, *15*, 2216–2220.
- [26] J. D. Goodreid, K. Wong, E. Leung, S. E. McCaw, S. D. Gray-Owen, A. Lough, W. A. Houry, R. A. Batey, *J. Nat. Prod.* **2014**, *77*, 2170–2181.
- [27] M. Gersch, K. Famulla, M. Dahmen, C. Göbl, I. Malik, K. Richter, V. S. Korotkov, P. Sass, H. Rübbsamen-Schaeff, T. Madl, H. Brötz-Oesterhelt, S. A. Sieber, *Nat. Commun.* **2015**, *6*, 6320.
- [28] M. Stahl, V. S. Korotkov, D. Balogh, L. M. Kick, M. Gersch, A. Pahl, P. Kielkowskij, K. Richter, S. Schneider, S. A. Sieber, *Angew. Chem. Int. Ed.* **2018**, *57*, 14602–14607; *Angew. Chem.* **2018**, *130*, 14811–14816.
- [29] J. D. Goodreid, E. da Silveira dos Santos, R. A. Batey, *Org. Lett.* **2015**, *17*, 2182–2185.
- [30] I. Ugur, M. Schroft, A. Marion, M. Glaser, I. Antes, *J. Mol. Model.* **2019**, *25*, 197.
- [31] D. A. Case, D. S. Cerutti, T. E. Cheatham, T. A. Darden, R. E. Duke, T. J. Giese, H. Gohlke, A. W. Goetz, D. Greene, N. Homeyer, S. Izadi, A. Kovalenko, T. S. Lee, S. LeGrand, P. Li, C. Lin, J. Liu, T. Luchko, R. Luo, D. Mermelstein, et al., *Amber 2017*, University of California, San Francisco, **2017**.
- [32] I. Antes, *Proteins Struct. Funct. Bioinf.* **2010**, *78*, 1084–1104.
- [33] Y. Perez-Riverol, A. Csordas, J. Bai, M. Bernal-Llinares, S. Hewapathirana, D. J. Kundu, A. Inuganti, J. Griss, G. Mayer, M. Eisenacher, E. Pérez, J. Uszkoreit, J. Pfeuffer, T. Sachsenberg, S. Yilmaz, S. Tiwary, J. Cox, E. Audain, M. Walzer, A. F. Jarnuczak, et al., *Nucleic Acids Res.* **2019**, *47*, D442–D450.

Manuscript received: August 2, 2019

Accepted manuscript online: September 5, 2019

Version of record online: January 7, 2020